AERODYNAMIC CHARACTERISTICS IN GROUND PROXIMITY

James L. Thomas, James L. Hassell, Jr.,
and Luat T. Nguyen
NASA Langley Research Center

SUMMARY

Results from recent investigations in the Langley V/STOL tunnel of an externally blown t_ n and an upper-surface blown flap configuration in ground proximity are presented. Comparisons of longitudinal aerodynamic characteristics indicate that in ground proximity, drag is reduced for both configurations, but changes in lift are configuration dependent. Steady-state analyses of the landing approach indicate an increase in flight-path angle for both configurations in ground proximity because of the drag reduction. Dynamic analyses with a fixed-base simulator indicate that the resultant flight path during landing approach is dependent on the initial flight-path angle and the control technique used.

Effects of asymmetries, such as sideslip or roll and engine-out characteristics, in ground proximity were also available from the wind-tunnel tests. Sideslip characteristics were generally unaffected by ground proximity. Roll attitudes were unstable at heights near gear touchdown height, and no significant yaw-roll coupling was noted. Engine-out characteristics were unaffected by ground proximity.

INTRODUCTION

In 1969, an investigation (ref. 1) was conducted in the 17-foot test section of the Langley 300-MPH 7- by 10-foot tunnel to determine the aerodynamic characteristics in ground proximity of the four-engine externally blown flap (EBF) configuration shown in figure 1. Various combinations of the segmented full-span double-slotted flaps were tested. Typical flap deflections were 30° in a take-off configuration and 60° in a landing configuration. Both high and low positions of the wing were tested. Changes in lift, drag, and pitching moment in ground proximity were measured over a moving ground belt.

The results from that investigation were used as the basis for a study presented at the STOL Technology Conference in 1972 (ref. 2) of ground proximity effects on powered-lift landing performance. The conclusions of that study were that the lift loss in ground proximity for most powered-lift configurations could be correlated with the height of the flap trailing edge and the level of developed lift. The lift loss increased as the trailing edge of the flap approached

the ground and increased with increasing lift coefficient. The "adverse" ground effect was, therefore, greater for low-wing configurations. Steady-state and in-flight simulator analyses indicated that acceptable landings could be made with conventional applications of power and elevator although the landing task was more difficult for a low-wing as opposed to a high-wing configuration.

Since aerodynamic characteristics are a function of the height above the ground, there is a need to assess possible adverse effects of airplane position asymmetries, such as sideslip or bank angle, in ground proximity which might be critical during the landing approach. For the example of an airplane banked in ground proximity, the lift loss might increase on the wing closer to the ground and be reduced on the higher wing, thereby causing a rolling moment into the ground beyond the available control power. This consideration led to tests in the Langley V/STOL tunnel of the EBF model shown in figure 2. The model is a four-engine configuration with full-span triple-slotted flaps very similar in planform to the earlier EBF model tested. Flap trailing-edge deflection angles were 40° in a take-off configuration and 55° in a landing configuration. Forces and moments were measured over a moving ground belt with a boundary-layer removal system in the front of the test section over a range of test conditions. The tests allowed an assessment of the effect of airplane position asymmetries, including roll angle, sideslip angle, and combined roll and sideslip angles, in ground proximity as well as a comparison of longitudinal characteristics in ground proximity with those for the earlier EBF configuration.

The upper-surface blown (USB) concept is a rather different type of powered-lift concept for which little data in ground proximity are available and which might have unexpected changes in aerodynamic characteristics near the ground, particularly with one engine inoperative. This consideration led to tests in the Langley V/STOL tunnel over a moving ground belt of the USB model shown in figure 3. The model is the twin-engine configuration discussed by Phelps, Johnson, and Margason in reference 3. Trailing-edge deflection angles of the Coanda flap behind the engines were 20° in a take-off configuration and 60° in a landing configuration. Outboard of the Coanda flaps were double-slotted flaps and a blown drooped aileron. The wind-tunnel results allowed an assessment of the longitudinal and engine-out characteristics of the USB configuration.

This paper thus updates the previous study on powered-lift aerodynamics in ground proximity with recent research results in the V/STOL tunnel. Comparisons of longitudinal aerodynamic characteristics for the EBF and for the USB configurations in ground proximity are possible. Steady-state and dynamic analyses of the landing approach for a typical STOL airplane are made to indicate the consequences of the aerodynamic changes in ground proximity.

SYMBOLS

Measurements and calculations were made in U.S. Customary Units and are presented in both the International System of Units (SI) and U.S. Customary Units.

146

A	aspect ratio
b	wing span, m (ft)
C_D	drag coefficient
ΔC_D	incremental drag coefficient, $C_D - C_{D,\infty}$
C_L	lift coefficient
ΔC_L	incremental lift coefficient, $C_L - C_{L,\infty}$
C_l	rolling-moment coefficient
$C_{l\beta}$	effective dihedral parameter
C_m	pitching-moment coefficient
C_n	yawing-moment coefficient
$C_{n\beta}$	directional stability parameter
C_μ	static thrust coefficient
h	height of wing quarter-chord above ground, m (ft)
I_Y	moment of inertia about pitch axis, kg-m^2 (slug-ft^2)
m	mass, kg, (slugs)
V	velocity, m/sec (ft/sec)
α	angle of attack, deg
β	angle of sideslip, deg
γ	flight-path angle, deg
δ_f	flap deflection angle, deg
$\Lambda_{c/4}$	sweep angle at wing quarter-chord, deg
λ	taper ratio
ϕ	bank angle, deg

Subscripts:

o	initial value
∞	free-air condition

Abbreviations:

BLC   boundary-layer control

EBF   externally blown flap

L.E.   leading edge

USB   upper-surface blown

LONGITUDINAL AERODYNAMIC CHARACTERISTICS IN GROUND PROXIMITY

Both the EBF and the USB models tested in the Langley V/STOL tunnel were sting supported over a moving ground belt with a boundary-layer removal system ahead of the belt. However, the ground belt was not available during most of the EBF tests, although the boundary-layer removal system was always available. The variation of lift coefficient with the height-span ratio h/b is presented with the boundary-layer removal system operating and with the ground belt on and off. Results are presented for the EBF and USB models in the take-off configuration at constant angle of attack through a range of thrust coefficient. The shaded area represents the conditions given by Turner (ref. 4) for which a moving ground belt is required to simulate ground proximity correctly. The results indicate a slightly lower level of lift without the belt operating at free-stream velocity, although the trends are predicted very well. For the range of lift coefficient and height-span ratio, the ground proximity can be properly simulated with only a boundary-layer removal system in the test section.

The longitudinal characteristics in ground proximity of the recently tested EBF $\left(\delta_f = 55^\circ\right)$ and USB $\left(\delta_f = 60^\circ\right)$ models and the previously tested EBF $\left(\delta_f = 60^\circ\right)$ model are presented in figure 5. The longitudinal forces and moments are presented as a function of h/b at constant angle of attack and at thrust coefficients appropriate for a free-air lift coefficient of about 4.25. Both EBF configurations show similar lift losses in ground proximity. The USB configuration shows a slight lift increase in ground proximity before losing lift at the lower heights. The lift is concentrated at the inboard sections of the wing for the USB configuration, whereas the lift is spread more outboard on the span for the EBF configurations. The differences in lift distribution may acco·t for some of the differences in lift in ground proximity, although there are als· differences in sweep between the configurations. Both EBF models are swept back 25° at the quarter-chord and the USB configuration is unswept. All three configurations, however, show a decrease in drag associated with the reduction in jet deflection angle as the ground is approached.

The pitching-moment data of figure 5 are untrimmed at different settings of tail incidence and are presented only to show the trends in ground proximity. The EBF models show nose-down moment increments in ground proximity and the pilot will have to exert trim control during landing. The trim control is usually obtained from a download at the tail, so that the trimmed lift loss in

148

ground proximity is increased. The USB configuration indicates only a slight nose-down moment in ground proximity. The sweep differences between the configurations are probably the cause of the differences in pitching moment.

Presented in figure 6 are lift and drag as a function of height-span ratio for the EBF and USB configurations tested in the V/STOL tunnel. Results are presented with the flaps at reduced deflections corresponding to take-off conditions at two values of thrust coefficient. At the reduced flap settings the lift and drag in ground proximity change significantly less even though the lift levels are comparable to those given in figure 5 for the landing configuration. The pitching-moment changes, although not presented, were also reduced with the lower flap deflections.

ANALYSIS OF LANDING APPROACH

The changes in aerodynamic characteristics in ground proximity are most critical during the landing approach and the effects of these changes are considered in both steady-state and dynamic analyses. The aerodynamic inputs were those forces and moments measured in the Langley V/STOL tunnel for the EBF and USB configurations in ground proximity. Trimmed lift and drag polars in ground proximity were constructed and a typical variation of trimmed lift and drag in ground proximity, nondimensionalized by the free-air lift coefficient, are shown in the left side of figure 7. Flight-path angle and angle of attack in ground proximity for a constant-thrust, constant-speed approach corresponding to a trimmed lift coefficient of 4.0 and initial flight-path angle of -6° are shown on the right side of figure 7. The results indicate that the reductions in drag more than offset any of the lift changes to increase the flight-path angle in ground proximity. The angle of attack must be reduced slightly for the USB configuration and increased slightly for the EBF configuration to maintain constant trimmed lift. A similar increase in flight-path angle in ground proximity was noted at the 1972 STOL Technology Conference (ref. 2). Reductions of the flight-path angle to zero in a flaring maneuver were possible with application of elevator and power.

The steady-state analysis of the landing approach assumes that force and moment changes in ground proximity translate directly into flight-path changes. However, the mass and inertial characteristics must be considered in a dynamic analysis to properly simulate the actual airplane landing approach. The mass and inertial characteristics of a typical STOL aircraft (m = 24 993 kg (1711 slugs) and I_Y = 334 642 kg-m^2 (246 819 slug-ft^2)) were used as input to the fixed-base dynamic simulation program of reference 5. Approaches were simulated over a range of initial flight-path angle, free-air lift coefficient, and control technique. The fixed-base simulator results for a constant-thrust approach using a feedback control from the elevator to maintain speed are shown in figure 8 for the EBF and USB configurations. Free-air trimmed lift coefficient is 4.27 and results are presented as flight-path trajectories for initial flight-path angles of -6° and -1.5°. At the higher rate of descent, the steady-state results do not have time to influence the flight path, and neither the USB nor the EBF configuration deviates much from the initial flight path. As

a check on the results, the analysis was continued below gear touchdown height and eventually the flight-path angle was increased corresponding to the steady-state results. At the lower rate of descent, the changes in forces and moments in ground proximity have a chance to develop and both configurations perform self-flaring maneuvers at ground heights near 6.1 m (20 ft).

The flight-path changes in ground proximity are dependent on the particular type of feedback control system used. The results for a constant-thrust approach using a feedback control from the elevator to maintain attitude are shown in figure 9. Neither configuration deviates from the steep flight path in ground proximity. At the lower initial rate of descent, the USB configuration performs a self-flaring maneuver near 4.9 m (16 ft). The EBF configuration does not flare, although it never falls below the initial flight-path trajectory.

The drag reductions in ground proximity common to both the EBF and the USB configurations are most important in determining steady-state flight-path increases in ground proximity. The lift changes are configuration dependent and the extent to which the steady-state results are experienced on the actual airplane depends on the initial flight-path angle and the particular type of f 'back control system used. None of the above analyses consider the flare m. uver which can be effected by application of either power or elevator.

SIDESLIP AND ROLL IN GROUND PROXIMITY

The EBF model in figure 2 was tested in the Langley V/STOL tunnel to determine the effect of sideslip angle, bank angle, and combined sidesiln and bank angles in ground proximity. Results in figure 10 for the pure sideslip condition in ground proximity are presented as effective dihedral $\left(-C_{l_\beta}\right)$ and directional stability $\left(C_{n_\beta}\right)$ as functions of height-span ratio for several thrust coefficients at constant angle of attack. Through sideslip angles of $\pm 10^\circ$, the EBF model indicated strong stability with little change due to ground proximity. The directional stability shows the expected increase with thrust because of the increased dynamic pressure at the tail. The effective dihedral is increased slightly at the lower height-span ratios.

The effect of roll in ground proximity is presented in figure 11 at a constant angle of attack and constant thrust corresponding to a free-air lift coefficient near 4.0. Rolling moment as a function of height-span ratio is presented for various roll attitudes. The pure roll case is shown on the left side of the figure, and positive bank angles corresponding to right wing down give large unstable rolling moments at height-span ratios near gear touchdown height. The combined roll and sideslip condition is given in the right side of the figure. The increment in rolling moment due to sideslip at $\phi = 0^\circ$ arises from the strong positive effective dihedral. Positive and negative roll attitudes give unstable rolling moments at height-span ratios near gear touchdown height. The unstable rolling-moment increment due to roll attitude is about the same at $\beta = 0^\circ$ and $\beta = -10^\circ$, indicating no significant yaw-roll coupling.

ENGINE-OUT CHARACTERISTICS IN GROUND PROXIMITY

The lateral-directional characteristics of the twin-engine USB concept in the event of engine failure during a powered-lift approach have been a matter of some concern. A concerted effort has been made to develop lateral control systems for this concept sufficiently powerful to trim out lateral asymmetries due to engine failure. Figure 12 illustrates the effect of engine failure in ground proximity. Results are presented in terms of yawing moment and rolling moment as functions of angle of attack for both the free-air condition (h/b = ∞) and in ground proximity (h/b = 0.2). The results presented are for the landing configuration $\left(\delta_f = 60^\circ\right)$ with the left engine inoperative and with the right engine at full thrust $\left(C_\mu = 1.80\right)$. The left side of figure 12 illustrates engine-out characteristics with all controls neutral. Surprisingly, the rolling-moment asymmetry was unaffected by ground proximity; however, the adverse yawing moment due to engine failure was reduced at the higher values of angle of attack.

The right side of figure 12 illustrates a possible solution to the lateral asymmetry problem due to engine failure. The aileron on the engine-out side has been drooped 60° and is augmented with blowing boundary-layer control (BLC). Also, the entire leading edge of the wing on the engine-out side is augmented with BLC to prevent flow separation at higher angles of attack. The results indicate that most of the rolling-moment asymmetry due to engine failure can be trimmed out with this lateral control system and that ground proximity had essentially no effect on the rolling-moment trim capability. Adverse yawing moment due to this lateral control is, in general, very slight (compare left- and right-hand yawing-moment data), and ground proximity causes the same reduction in yawing-moment asymmetry at higher values of angle of attack as was observed with lateral controls neutral. It should be mentioned that the twin-engine USB concept requires a double-hinged rudder capable of handling the yawing moments due to engine failure during take-off, and such a rudder control would be more than adequate to trim out the yawing moments shown in figure 12 for the landing configuration.

CONCLUSIONS

The following conclusions are drawn from the recent wind-tunnel investigations of powered-lift configurations:

1. Drag reductions in ground proximity are common to both EBF and USB configurations, whereas changes in lift are configuration dependent.

2. The extent to which the predicted steady-state flight-path increases in ground proximity are experienced on the actual airplane depends on the initial flight-path angle and the control technique used.

3. Lateral-directional characteristics due to sideslip are unaffected by ground proximity, whereas roll attitudes give unstable rolling moments near gear touchdown height.

4. Engine-out characteristics both with and without corrective control are unaffected by ground proximity.

REFERENCES

1. Vogler, Raymond D.: Wind-Tunnel Investigation of a Four-Engine Externally Blowing Jet-Flap STOL Airplane Model. NASA TN D-7034, 1970.

2. Hassell, James L., Jr.; and Judd, Joseph H.: Study of Ground Proximity Effects on Powered-Lift STOL Landing Performance. STOL Technology, NASA SP-320, 1972, pp. 199-213.

3. Phelps, Arthur E., III; Johnson, Joseph L., Jr.; and Margason, Richard J.: Summary of Low-Speed Aerodynamic Performance of the Upper-Surface-Blown Jet-Flap Concept. Powered-Lift Aerodynamics and Acoustics, NASA SP-406, 1976. (Paper no. 4 of this compilation.)

4. Turner, Thomas R.: Endless-Belt Technique for Ground Simulation. Conference on V/STOL and STOL Aircraft, NASA SP-116, 1966, pp. 435-446.

5. Grantham, William D.; Nguyen, Luat T.; Patton, James M., Jr.; Deal, Perry L.; Champine, Robert A.; and Carter, C. Robert: Fixed-Base Simulator Study of an Externally Blown Flap STOL Transport Airplane During Approach and Landing. NASA TN D-6898, 1972.
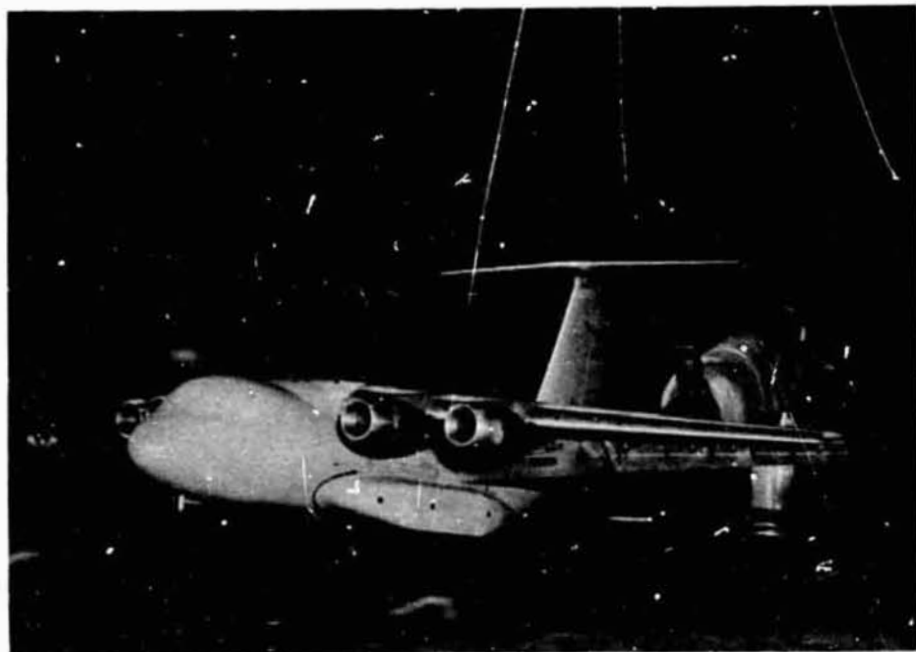
Figure 1.- EBF configuration tested in 17-foot test section of Langley 300-MPH 7- by 10-foot tunnel. $A = 7.0$; $\Lambda_{c/4} = 25^o$; $\lambda = 0.3$.
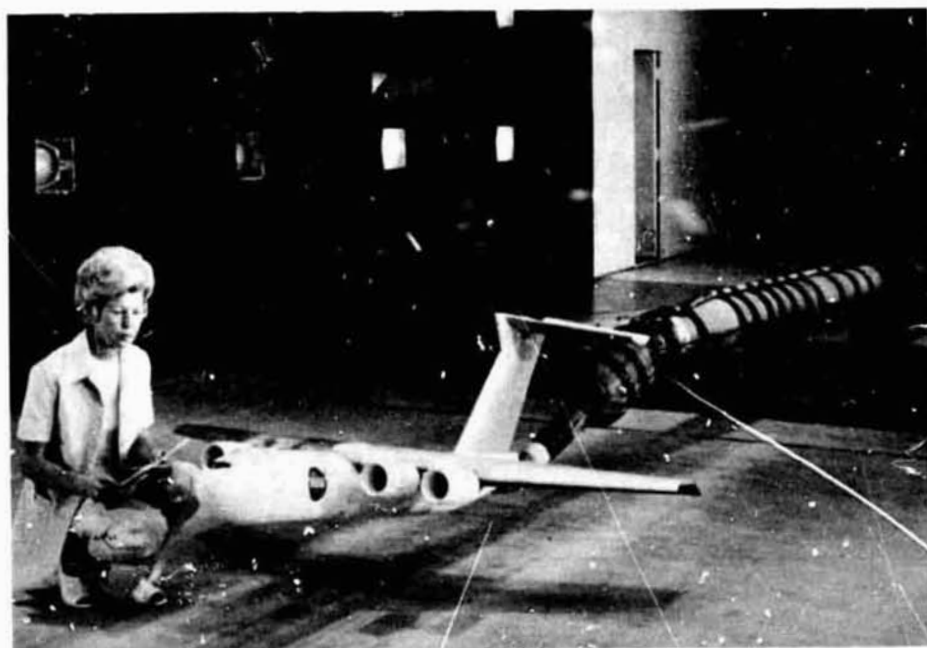
Figure 2.- EBF configuration tested in Langley V/STOL tunnel. $A = 7.3$; $\Lambda_{c/4} = 25^o$; $\lambda = 0.4$.
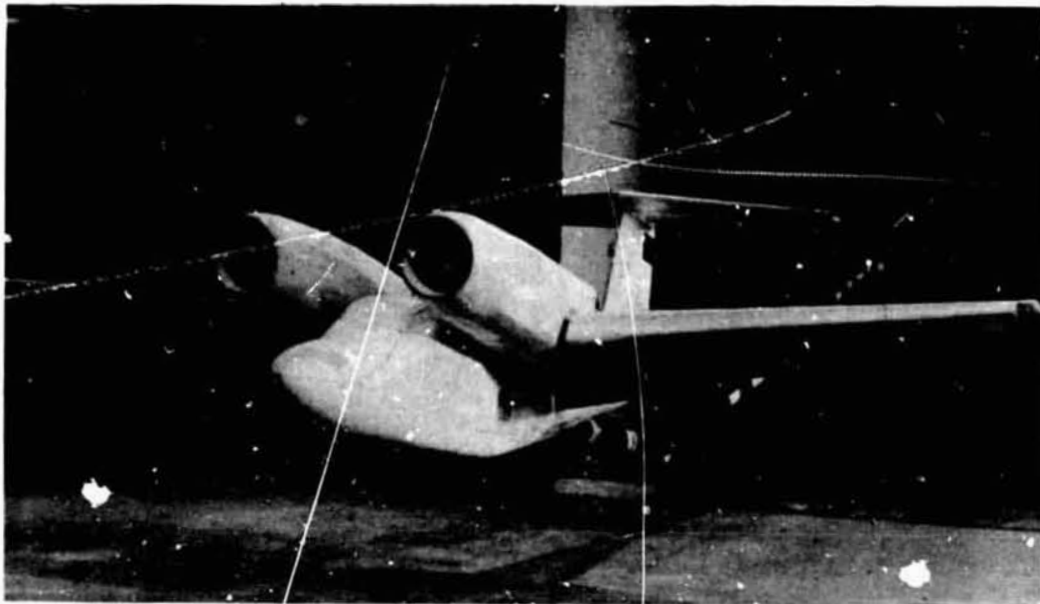
Figure 3.- USB configuration tested in Langley V/STOL tunnel.
A = 8.2; $\Lambda_{c/4}$ = 0°; λ = 0.3.
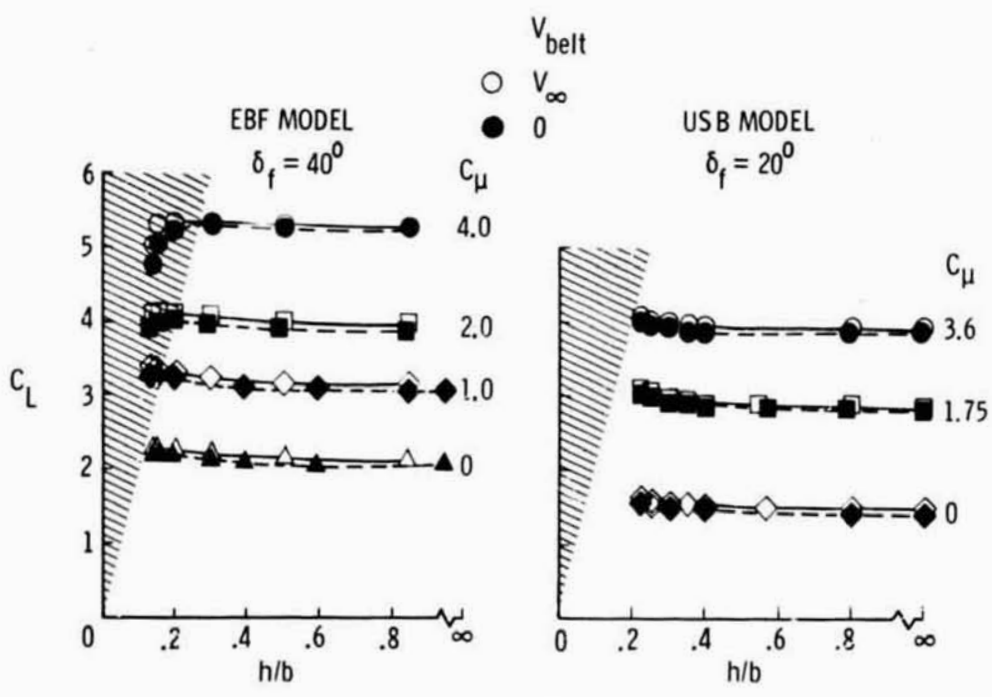
Figure 4.- Effect of moving ground belt on lift in ground
proximity with boundary-layer removal system operating.
α = 5°.
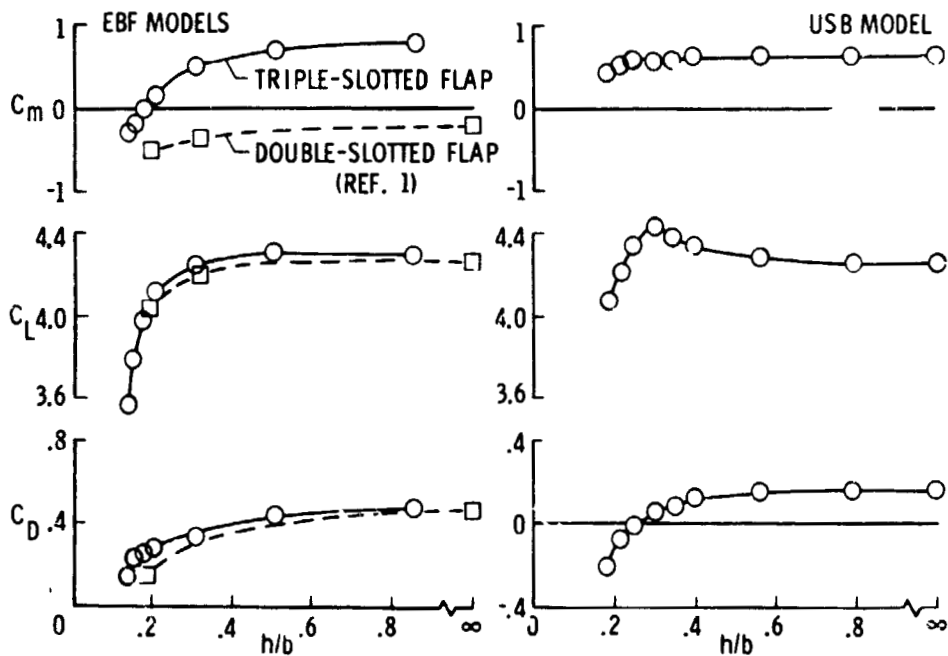
Figure 5.- Ground effect on longitudinal aerodynamics of landing configurations. $\alpha = 5^{o}$; C_μ = Constant; $C_{L,\infty} = 4.25$.
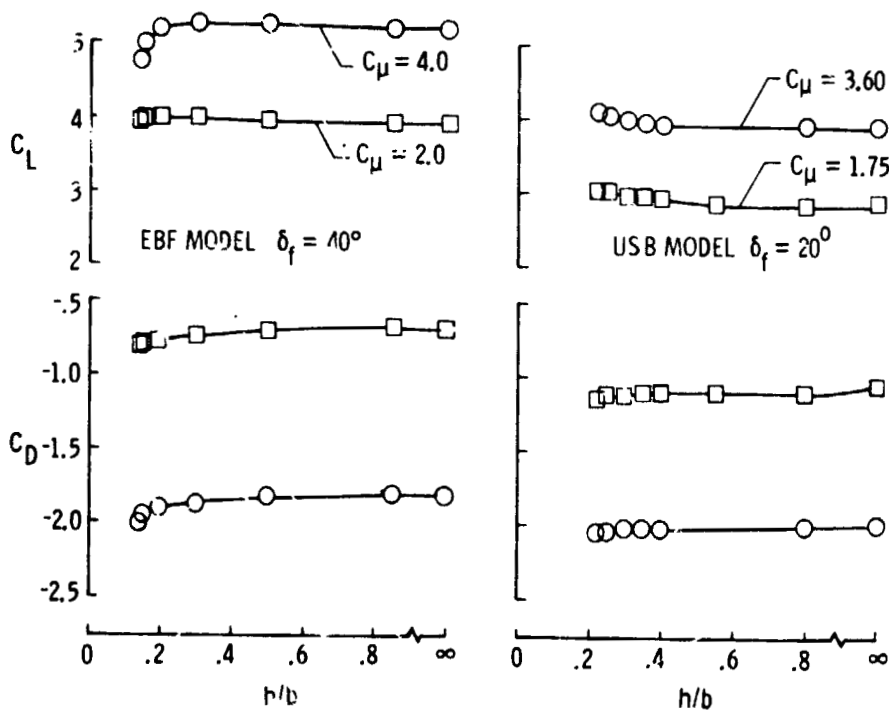
Figure 6.- Ground effect on longitudinal aerodynamics of take-off configurations. $\alpha = 5^{o}$.
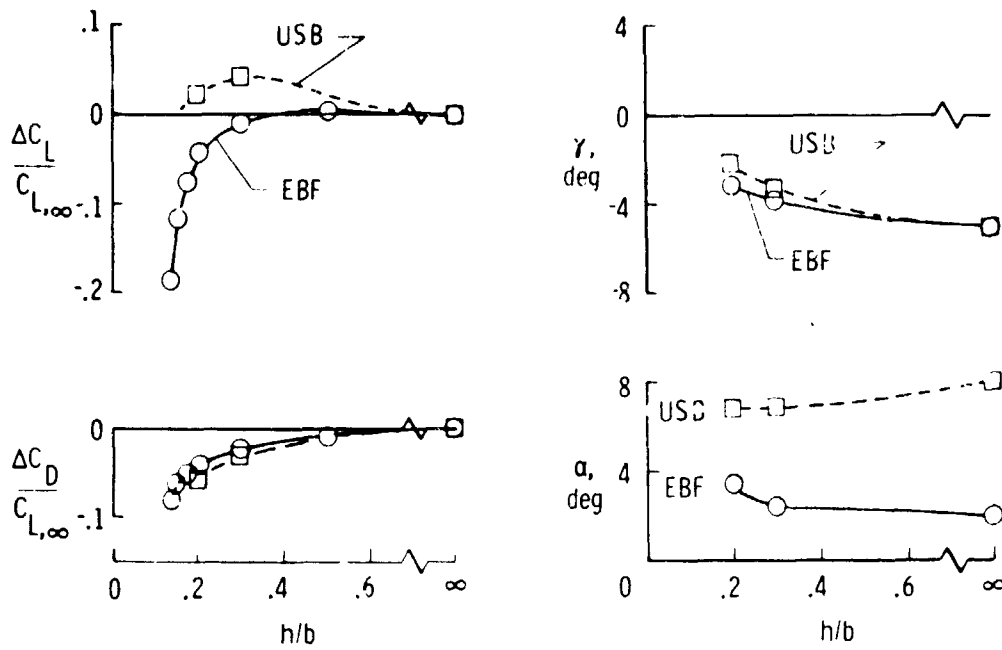
Figure 7.- Results from steady-state analysis of constant-thrust, constant-speed landing approach. $C_{L,trim} = 4.0$.
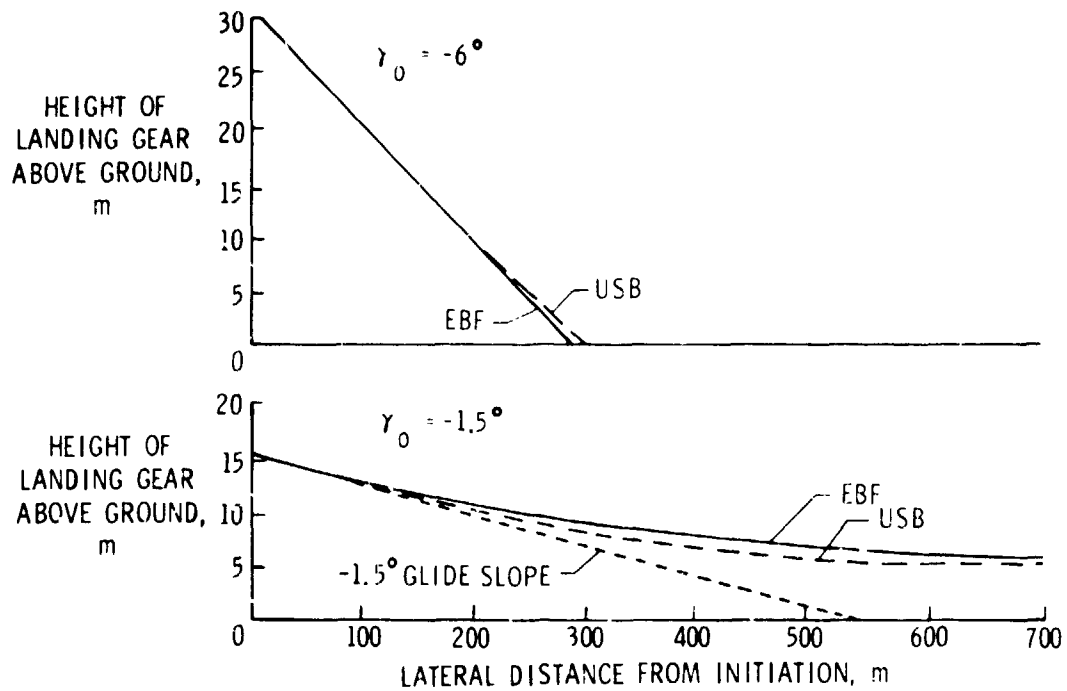
Figure 8.- Results from fixed-base simulator analysis of constant-thrust, constant-speed landing approach using elevator control. $(C_{L,trim})_\infty = 4.27$.
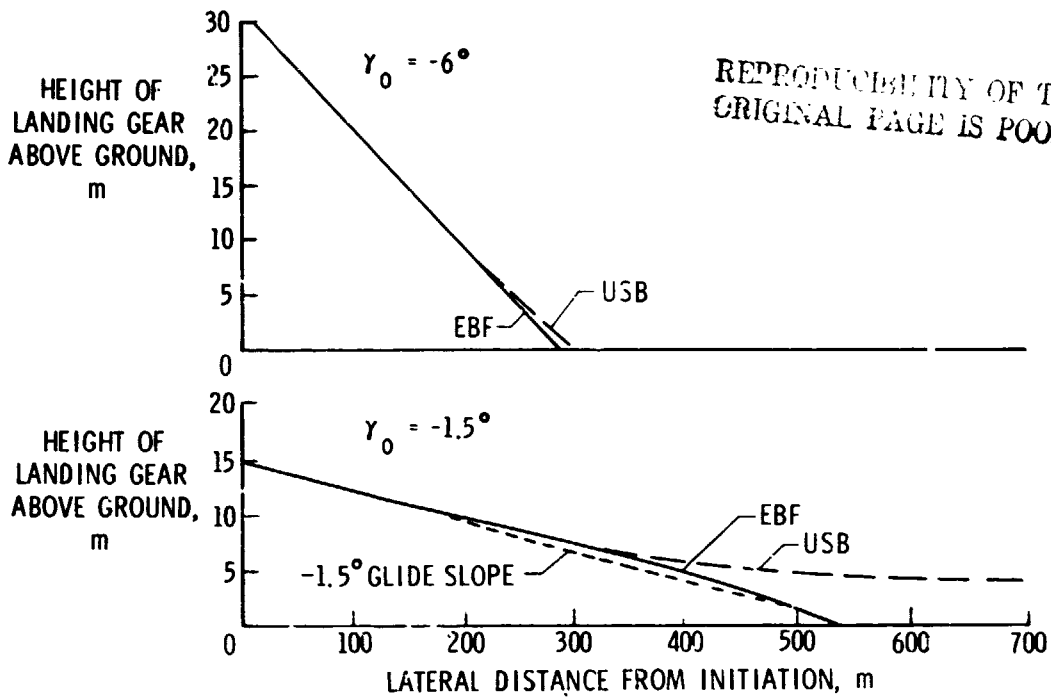
Figure 9.- Results from fixed-base simulator analysis of constant-thrust, constant-attitude landing approach using elevator control. $\left(C_{L,trim}\right)_{\infty} = 4.27$.
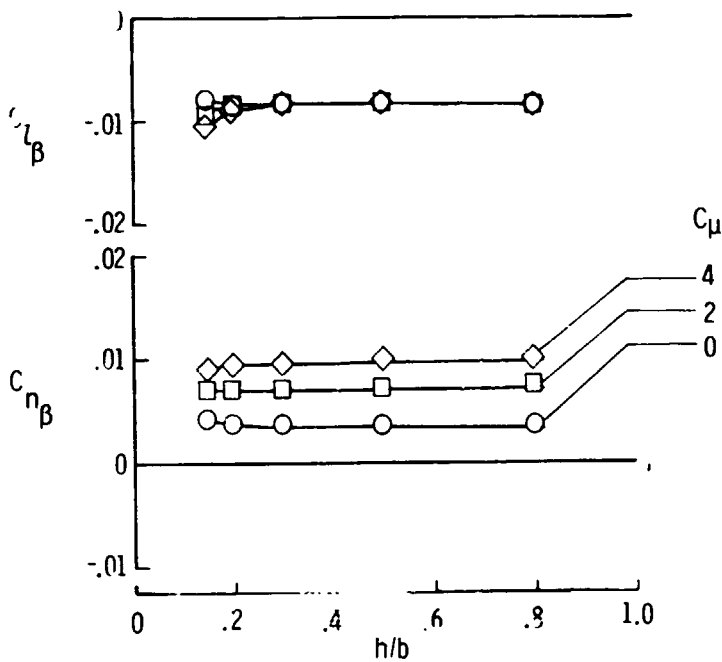
Figure 10.- Static lateral-directional characteristics in ground proximity. Triple-slotted EBF model; $\delta_f = 40^{\circ}$; $\alpha = 5^{\circ}$

157
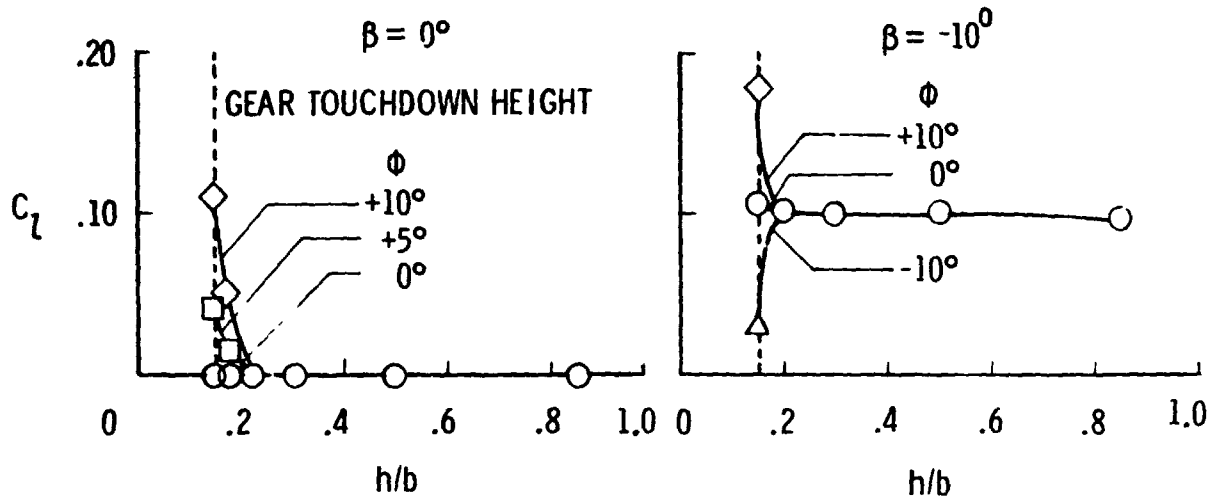
Figure 11.- Effect of bank angle in ground proximity. Triple-slotted EBF model; $\delta_f = 40°$; $\alpha = 5°$; $C_\mu = 2$; $C_{L,\infty} = 4.0$.
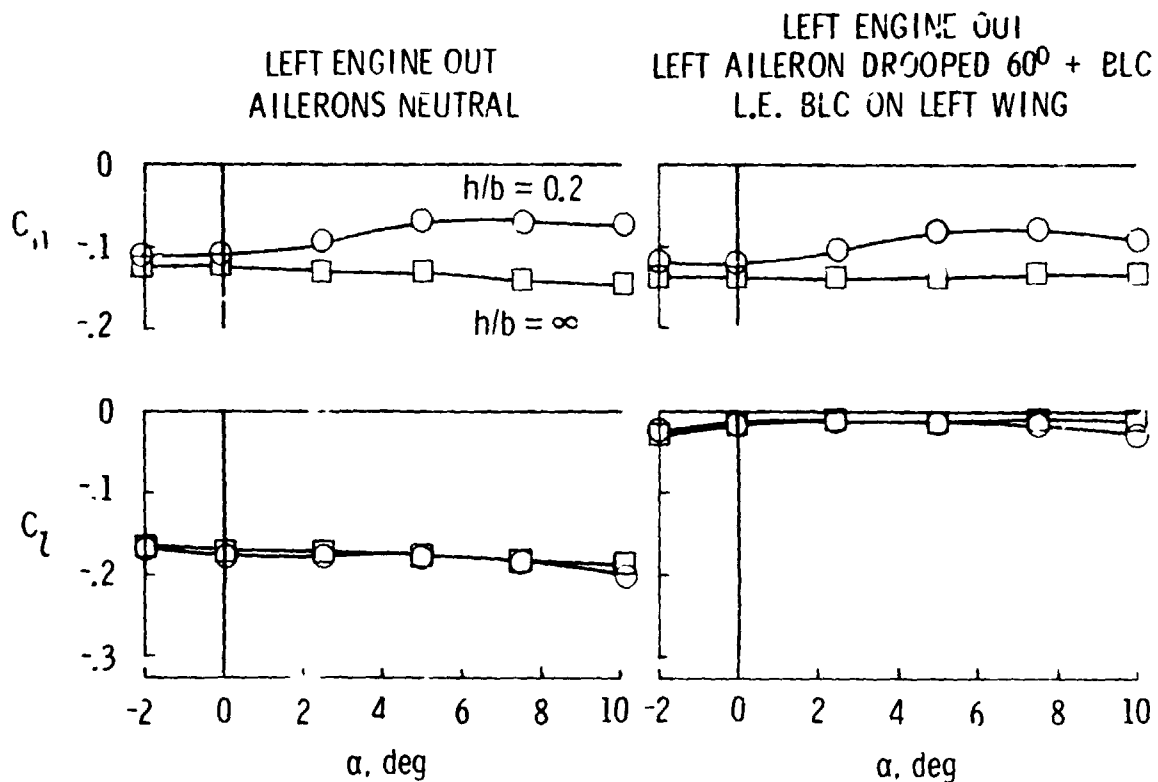
Figure 12.- Engine-out characteristics in ground proximity. Twin-engine USB configuration; $C_\mu = 1.80$; left engine out; $\delta_f = 60°$.